

# On the use of *Gaia* magnitudes and new tables of bolometric corrections

L. Casagrande<sup>1,2★</sup> and Don A. Vandenberg<sup>3</sup>

<sup>1</sup>Research School of Astronomy and Astrophysics, Mount Stromlo Observatory, The Australian National University, Canberra, ACT 2611, Australia

<sup>2</sup>ARC Centre of Excellence for All Sky Astrophysics in 3 Dimensions (ASTRO 3D), Canberra, Australia

<sup>3</sup>Department of Physics & Astronomy, University of Victoria, PO Box 1700 STN CSC, Victoria, BC V8W 2Y2, Canada

Accepted 2018 June 6. Received 2018 June 01; in original form 2018 May 10

## ABSTRACT

The availability of reliable bolometric corrections and reddening estimates, rather than the quality of parallaxes, will be one of the main limiting factors in determining the luminosities of a large fraction of *Gaia* stars. With this goal in mind, we provide *Gaia*  $G_{BP}$ ,  $G$ , and  $G_{RP}$  synthetic photometry for the entire MARCS grid and test the performance of our synthetic colours and bolometric corrections against space-borne absolute spectrophotometry. We find indication of a magnitude-dependent offset in *Gaia* DR2  $G$  magnitudes, which must be taken into account in high-accuracy investigations. Our interpolation routines are easily used to derive bolometric corrections at desired stellar parameters and to explore the dependence of *Gaia* photometry on  $T_{\text{eff}}$ ,  $\log g$ ,  $[\text{Fe}/\text{H}]$ ,  $[\alpha/\text{Fe}]$ , and  $E(B - V)$ . *Gaia* colours for the Sun and Vega, and  $T_{\text{eff}}$ -dependent extinction coefficients are also provided.

**Key words:** techniques: photometric – stars: atmospheres – stars: fundamental parameters – stars: Hertzsprung–Russell and colour–magnitude diagrams.

## 1 INTRODUCTION

*Gaia* DR2 includes photometry in the  $G_{BP}$ ,  $G$ , and  $G_{RP}$  bands for approximately 1.5 billion sources. Its exquisite quality will define the new standard in the years to come and have a tremendous impact on various areas of astronomy. The first goal of this letter is to lay out the formalism to generate *Gaia* magnitudes from stellar fluxes, using the official *Gaia* zero-points and transmission curves (Evans et al. 2018). In doing so, we discuss in some detail the effect of different zero-points and search for an independent validation of the results using space-based spectrophotometry.

One of the important prerequisites for stellar studies is the availability of *Gaia* colour transformations and bolometric corrections (BCs) to transpose theoretical stellar models onto the observational plane and to estimate photometric stellar parameters including luminosities. In Casagrande & Vandenberg (2014, 2018, hereafter Papers I and II) we have initiated an effort to provide reliable synthetic colours and BCs from the MARCS library of theoretical stellar fluxes (Gustafsson et al. 2008) for different combinations of  $T_{\text{eff}}$ ,  $\log g$ ,  $[\text{Fe}/\text{H}]$ ,  $[\alpha/\text{Fe}]$ , and  $E(B - V)$ . Here, we extend that work to include the *Gaia* system. We also provide extinction coefficients and colours for Vega and the Sun, both being important calibration points for a wide range of stellar, Galactic, and extragalactic astronomy.

## 2 THE *Gaia* SYSTEM

The precision of *Gaia* photometry is better than that of any other currently available large catalogues of photometric standards; hence its calibration is achieved via an internal self-calibrating method (Carrasco et al. 2016). This robust internal photometric system is then tied to the Vega system by means of an external calibration process that uses a set of well-observed spectro-photometric standard stars (Pancino et al. 2012; Altavilla et al. 2015). Observationally, a *Gaia* magnitude is defined as

$$m_{\zeta} = -2.5 \log \bar{I}_{\zeta} + ZP_{\zeta}, \quad (1)$$

where  $\bar{I}_{\zeta}$  is the weighted mean flux in a given band  $\zeta$  (i.e.  $G_{BP}$ ,  $G$ , or  $G_{RP}$ ) and  $ZP_{\zeta}$  is the zero-point to pass from instrumental to observed magnitudes (Carrasco et al. 2016). Zero-points are provided to standardize *Gaia* observations to the Vega ( $ZP_{\zeta, \text{VEGA}}$ ) or AB ( $ZP_{\zeta, \text{AB}}$ ) systems. The weighted mean flux measured by *Gaia* for a spectrum  $f_{\lambda}$  can be calculated from

$$\bar{I}_{\zeta} = \frac{P_A}{10^9 h c} \int \lambda f_{\lambda} T_{\zeta} d\lambda, \quad (2)$$

where  $P_A$  is the telescope pupil area,  $T_{\zeta}$  the bandpass,  $h$  the Planck constant, and  $c$  the speed of light in vacuum (see Evans et al. 2018 for the units of measure in each term). While  $T_{\zeta}$ ,  $ZP_{\zeta, \text{VEGA}}$ , and  $ZP_{\zeta, \text{AB}}$  are the quantities used to process and publish the *Gaia* DR2 photometry, Evans et al. (2018) also provide a revised set of transmission curves and zero-points ( $T_{\zeta}^R$ ,  $ZP_{\zeta, \text{VEGA}}^R$ , and  $ZP_{\zeta, \text{AB}}^R$ ). Here, we have generated synthetic photometry using both sets, and call them “processed” (*Gaia-pro*) and “revised” (*Gaia-rev*). Although the revised transmission curves and zero-points provide a better charac-

\* E-mail: luca.casagrande@anu.edu.au

terization of the satellite system, DR2 magnitudes were not derived using them. To account for this inconsistency, the published DR2 Vega magnitudes should be shifted by  $-ZP_{\zeta,VEGA} + ZP_{\zeta,VEGA}^R$  (Gaia Collaboration et al. 2018a). Since many users might overlook this minor correction (at the mmag level), we supply a third set of synthetic magnitudes that take it into account, by using  $ZP_{\zeta,VEGA}$  in equation (1) and  $T_{\zeta}^R$  in equation (2). We call these magnitudes Gaia-DR2 in our interpolation routines, and they should be preferred when comparing predicted colours with published DR2 photometry *as is*.

While we adopt the formalism of equations (1) and (2), we remark that from the definition of AB magnitudes (e.g. Paper I, where  $m_{\zeta,AB}$  or  $m_{\zeta,AB}^R$  indicates whether  $T_{\zeta}$  or  $T_{\zeta}^R$  is used to compute AB magnitudes), an alternative formulation to generate synthetic Gaia magnitudes in the Vega system would be  $m_{\zeta,AB} + ZP_{\zeta,VEGA} - ZP_{\zeta,AB}$  (Gaia-pro),  $m_{\zeta,AB}^R + ZP_{\zeta,VEGA}^R - ZP_{\zeta,AB}^R$  (Gaia-rev), and  $m_{\zeta,AB}^R + ZP_{\zeta,VEGA} - ZP_{\zeta,AB}^R$  (Gaia-DR2). These hold true if the Gaia zero-points in equation (1) provide exact standardization to the AB system. We verified that the magnitudes obtained with this alternative formulation versus Equations (1) and (2) are identical to  $<1$  mmag for Gaia-pro, and to 3 mmag for Gaia-rev and Gaia-DR2. Importantly, we note that, in no instance, have we used Gaia DR1 data, nor the pre-launch filter curves (Jordi et al. 2010) anywhere in this paper.

## 2.1 Check on zero-points

The CALSPEC<sup>1</sup> library contains composite stellar spectra that are flux standards in the *Hubble Space Telescope* (HST) system. The latter is based on three hot, pure hydrogen white dwarf standards normalized to the absolute flux of Vega at 5556 Å. The absolute flux calibrations of CALSPEC stars are regularly updated and improved, arguably providing the best spectrophotometry set available to date, with a flux accuracy at the (few) percent level (Bohlin 2014). In particular, the highest quality measurements in CALSPEC are obtained by the STIS (0.17–1.01  $\mu\text{m}$ ) and NICMOS (1.01–2.49  $\mu\text{m}$ ) instruments on board the HST.

By replacing  $f_{\lambda}$  in equation (2) with CALSPEC fluxes, it is thus possible to compute the expected  $G_{BP}$ ,  $G$ , and  $G_{RP}$  magnitudes for these stars to compare with those reported in the Gaia catalogue. For this exercise, we use only CALSPEC stars having STIS observations (i.e. covering the Gaia bandpasses). Further, we remove stars labelled as variable in CALSPEC and retain only Gaia magnitudes with the designation `duplicated_source=0`, `phot_proc_mode=0` (i.e. “Gold” sources, see Riello et al. 2018). We also remove a handful of stars with flux excess factors (a measure of the inconsistency between  $G_{BP}$ ,  $G$ , and  $G_{RP}$  bands typically arising from binarity, crowding, and incomplete background modelling) that are significantly higher than those of the rest of the sample (`phot_bp_rp_excess_factor < 1.3`). The resultant comparison is shown in Fig. 1. The differences between the computed and observed  $G_{BP}$  and  $G_{RP}$  magnitudes are only a few mmag. However,  $G$  magnitudes show a clear magnitude-dependent trend, which in fact is qualitatively in agreement with those shown in the left-hand panels of figs 13 and 24 by Evans et al. (2018). After taking into account the errors in the synthetic magnitudes from CALSPEC

flux uncertainties and Gaia measurements,<sup>2</sup> the significance of this slope is close to  $5\sigma$ . No trend is observed as function of colour. A constant offset between CALSPEC and Gaia synthetic magnitudes would indicate a difference in zero-points or absolute calibration, simply confirming intrinsic limitations on the current absolute flux scale (which linchpin on Vega’s flux at 5555 Å for CALSPEC and 5500 Å for Gaia). A drift of the CALSPEC absolute flux scale at fainter magnitudes would appear in all filters: the fact no trend is seen for  $G_{BP}$  nor  $G_{RP}$  magnitudes likely indicates that the cause of the problem stems from Gaia  $G$  magnitudes instead. The sign of this trend implies that Gaia  $G$  magnitudes are brighter than synthetic CALSPEC photometry for  $G \lesssim 14$ , although for a few stars this occurs at  $G \sim 12$ . Understanding the origin of this deviation is outside the scope of this letter. Here we provide a simple fit to place Gaia  $G$  magnitudes onto the same CALSPEC scale as for  $G_{BP}$  and  $G_{RP}$  magnitudes:

$$G^{\text{corr}} = 0.0505 + 0.9966 G, \quad (3)$$

which applies over the range  $6 \text{ mag} \lesssim G \lesssim 16.5 \text{ mag}$ . While brighter  $G$  magnitudes in Gaia are affected by saturation (the trend found by Evans et al. 2018 using *Tycho2* and *Hipparcos* photometry is also seen by us, see Fig. 1), it remains to be seen whether the offset that we find extends to magnitudes fainter than 16.5.

## 3 ON BOLOMETRIC CORRECTIONS AND OTHER UNCERTAINTIES ON STELLAR LUMINOSITIES

We refer to Papers I and II for a description of the MARCS grid, our interpolation routines, and examples of their use for different input reddenings (in all cases we have adopted the Cardelli, Clayton & Mathis 1989 parametrization of the extinction law). We also emphasize once more the importance of paying attention to the zero-point of the bolometric magnitude scale, which is arbitrary, but once chosen, must be abided. In our grid, there is no ambiguity in the zero-point of the BCs, which is instead an unnecessary source of biases when matching a synthetic grid to heterogeneous observations (Andrae et al. 2018). To derive BCs from our grid requires the prior knowledge of stellar parameters, which often might not be a trivial task. Our scripts easily allow one to test the effects on BCs of varying the input stellar parameters. Projecting BCs as function of  $T_{\text{eff}}$  would also be affected by the distribution of stellar parameters underlying the grid. In nearly all circumstances, this distribution would be different from that of the sample used for a given investigation.

In Papers I and II we carried out extensive tests of the MARCS synthetic colours and BCs against observations, concluding that observed broad-band colours are overall well reproduced in the range encompassed by the Gaia bandpasses, with the performance downgrading towards the blue and ultraviolet spectral regions. For the sake of this letter, we want to know how well bolometric fluxes can be recovered<sup>3</sup> from Gaia photometry. In fact, Gaia parallaxes deliver exquisite absolute magnitudes for a large fraction of stars

<sup>2</sup>In all instances, flux uncertainties from CALSPEC and Gaia are small enough that the skewness of mapping fluxes into magnitudes has no impact, but see appendix B of Paper I for a discussion of this effect.

<sup>3</sup>Bolometric flux ( $\text{erg s}^{-1} \text{cm}^{-2}$ ) implies the flux across the entire spectrum that an observer (us) would measure from a star at distance  $d$ . On the other hand, luminosity ( $\text{erg s}^{-1}$ ) refers to the intrinsic energy output of a star, i.e.  $4\pi d^2$  times the bolometric flux.

<sup>1</sup><http://www.stsci.edu/hst/observatory/crds/calspec.html>

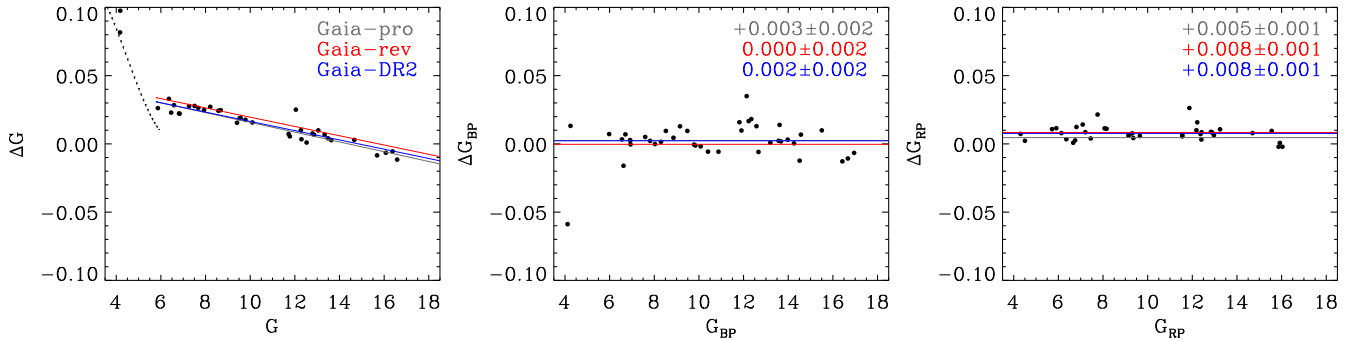


**Figure 1.** Residuals between synthetic photometry computed with the CALSPEC library and the corresponding *Gaia* magnitudes. Only the comparisons with the *Gaia*-DR2 synthetic magnitudes are shown, but nearly indistinguishable trends are obtained using *Gaia*-pro and *Gaia*-rev (see Section 2 for nomenclature). Median residuals and standard deviations of the mean are reported for all cases. The departure at  $G \sim 4$  (left-hand panel), which is not included as part of our fit, is likely due to the saturation of bright sources in *Gaia*. The dotted line in the left-hand panel is the correction at bright magnitudes from Evans et al. (2018, their equation B1).

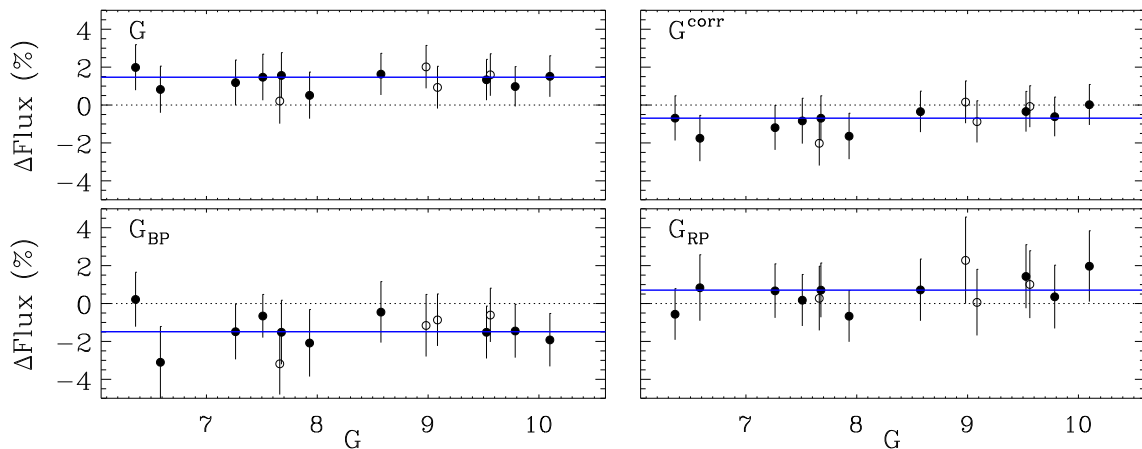


**Figure 2.** Percentage difference between bolometric fluxes from CALSPEC photometry, and those recovered from our BCs (bands indicated in the top left corner of each panel). The stars and parameters that were adopted in our interpolation routines are the same as in Table 2 of Paper II. Filled circles are stars satisfying quality requirements listed in Section 2.1. Open circles are stars with `duplicated_source=1` (which may indicate observational, cross-matching or processing problems, or stellar multiplicity, and probable astrometric or photometric problems in all cases). Errors bars are obtained assuming a fixed 1 per cent uncertainty in CALSPEC fluxes, and Monte Carlo simulations taking into account the quoted uncertainties in both the input stellar parameters and observed photometry for each target. Continuous blue lines indicate median offsets, dotted lines centred at zero are used to guide the eye. BCs from the *Gaia*-DR2 set are used in all instances, although nearly identical results are obtained using the *Gaia*-pro and *Gaia*-rev sets.

(Gaia Collaboration et al. 2018b). However, when comparing them with stellar models, one of the main limiting factors stems from the quality of the BCs. Here we extend the comparison of Table 2 in Paper II (which is limited by the availability of reliable stellar parameters to F and G dwarfs at various metallicities) to include *Gaia*  $G_{BP}$ ,  $G$ , and  $G_{RP}$  magnitudes. Our goal is to assess how well our BCs recover the bolometric fluxes measured from the CALSPEC library. This is shown in Fig. 2. The first thing to notice is the offset, as well as scatter associated with the BCs in  $G_{BP}$ . While the synthetic photometry presented in Fig. 1 only relies on the observed spectrophotometry and how well a bandpass is standardized, the quality of the comparison in Fig. 2 also depends on the MARCS models, as well as the input stellar parameters that were adopted when our tables of BCs were interpolated. As already mentioned, the performance of the MARCS models downgrades towards the blue, and in this spectral region stellar fluxes have a stronger dependence on stellar parameters. The comparison is better in  $G_{RP}$  band (bottom right) as well as in the  $G$  band (top panels). In the latter case, applying equation (3) to correct the *Gaia* photometry improves the

agreement, but it does not yield to a perfect match (for the same reasons that were just discussed). In all cases, the offset and scatter typically vary between 1 and 2 per cent, which we regard as the uncertainty of our BCs (0.01–0.02 mag for the F and G dwarfs tested here).

To summarize, we now estimate the fractional contribution of different uncertainties to stellar luminosities. Assuming systematic errors in magnitudes are under control (or corrected for, as we discussed), the precision of *Gaia* magnitudes  $\sigma_\zeta$  is typically at the mmag level (although larger for sources that are very bright, in crowded regions, or very faint) meaning they contribute with a negligible  $0.4 \ln(10) \sigma_\zeta$  to the luminosity error budget. Other contributions amount to  $0.4 \ln(10) R_\zeta \sigma_{E(B-V)}$  for reddening,  $0.4 \ln(10) \sigma_{BC}$  for BCs, and  $2\sigma_\omega/\omega$  for parallaxes. This implies that the uncertainty in BCs is dominant over the parallax error when  $\sigma_{BC} \gtrsim 2.2 \sigma_\omega/\omega$ . In other words, when parallaxes are better than 0.5 per cent, BCs are the dominant source of uncertainty if  $\sigma_{BC} \sim 0.01$ . This is shown by the purple line in Fig. 3, where the interplay among different uncertainties for a target luminosity error is explored.

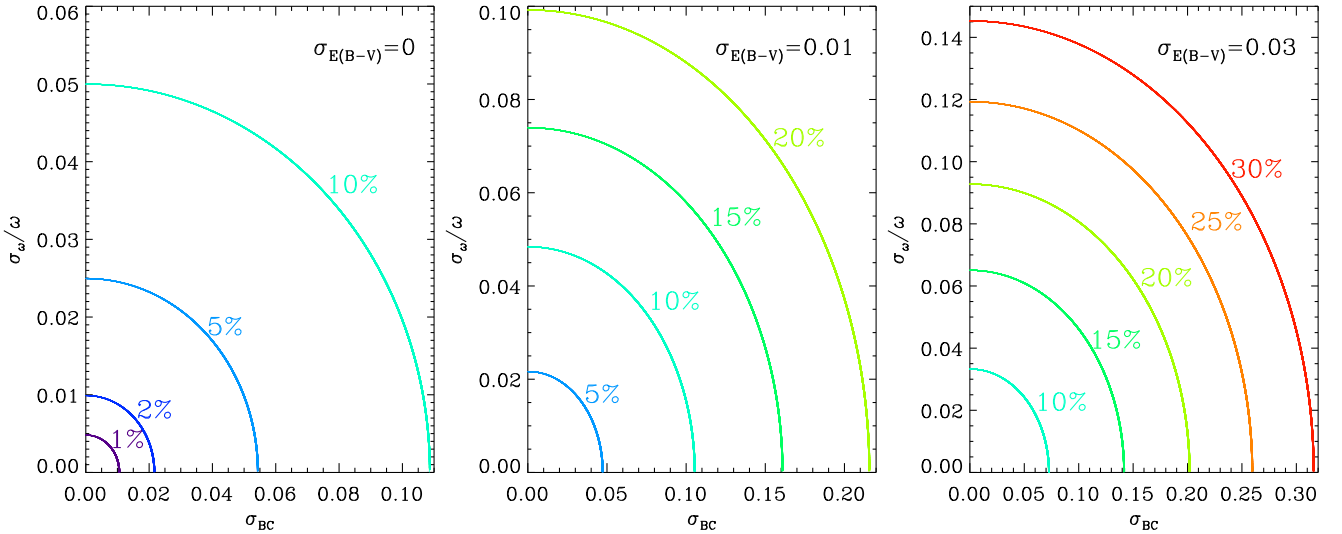


**Figure 3.** *Left-hand panel:* Correlation between the uncertainties in parallax ( $\sigma_\omega/\omega$ ) and BCs ( $\sigma_{BC}$ ) for a target precision in luminosity (indicated by different curves). Magnitude uncertainties are fixed at 3 mmag. *Middle and right-hand panels:* Same as the left-hand panel, but assuming a reddening uncertainty of 0.01 and 0.03 mag, respectively. An extinction coefficient of 2.7 is adopted (appropriate for the  $G$  band, and in between those for  $G_{BP}$  and  $G_{RP}$ ). The theoretical lower limit on the luminosity error is set by *Gaia* magnitudes in the left-hand panel ( $\sim 0.3$  per cent), and reddening in the central ( $\sim 2.5$  per cent) and right-hand ( $\sim 7.5$  per cent) panels.

**Table 1.** Predicted *Gaia* magnitudes and colours for the Sun and Vega in the Vega and AB systems. See Section 2 for a discussion of *Gaia-pro*, *Gaia-rev* and *Gaia-DR2* realizations, and Section 4 for a description of the spectral templates.

Object	Template	$G$	$G_{BP} - G$	$G - G_{RP}$	$G_{BP} - G_{RP}$	System	Realization	
Sun	sun_mod_001.fits	-26.792	0.257	0.241	0.498	AB	Gaia-pro	
		-26.792	0.261	0.237	0.498	AB	Gaia-rev	
		-26.897	0.333	0.490	0.823	Vega	Gaia-pro	
		-26.892	0.324	0.491	0.815	Vega	Gaia-rev	
		-26.895	0.329	0.488	0.818	Vega	Gaia-DR2	
		-26.792	0.257	0.242	0.499	AB	Gaia-pro	
	sun_reference_stis_002.fits	-26.791	0.261	0.238	0.500	AB	Gaia-rev	
		-26.897	0.333	0.491	0.824	Vega	Gaia-pro	
		-26.891	0.324	0.492	0.816	Vega	Gaia-rev	
		-26.894	0.330	0.489	0.819	Vega	Gaia-DR2	
		Thuillier et al.(2004)	-26.799	0.259	0.244	0.502	AB	Gaia-pro
			-26.798	0.263	0.240	0.503	AB	Gaia-rev
-26.904	0.335		0.493	0.828	Vega	Gaia-pro		
Vega	alpha_lyr_mod_002.fits	-26.898	0.326	0.493	0.819	Vega	Gaia-rev	
		-26.901	0.331	0.491	0.823	Vega	Gaia-DR2	
		0.140	-0.072	-0.238	-0.310	AB	Gaia-pro	
		0.134	-0.057	-0.243	-0.300	AB	Gaia-rev	
		0.035	0.004	0.011	0.015	Vega	Gaia-pro	
	alpha_lyr_stis_008.fits	0.034	0.006	0.010	0.016	Vega	Gaia-rev	
		0.031	0.011	0.008	0.019	Vega	Gaia-DR2	
		0.138	-0.073	-0.240	-0.313	AB	Gaia-pro	
		0.132	-0.058	-0.246	-0.304	AB	Gaia-rev	
		0.033	0.003	0.009	0.012	Vega	Gaia-pro	
	0.032	0.005	0.008	0.012	Vega	Gaia-rev		
	0.029	0.010	0.006	0.016	Vega	Gaia-DR2		

#### 4 THE COLOURS OF THE SUN AND VEGA

The solar colours provide an important benchmark point in many areas of astronomy and astrophysics. The least model dependent and arguably the best method to determine them relies on solar twins (Meléndez et al. 2010; Casagrande et al. 2012; Ramírez et al. 2012). Here we use instead the formalism developed for *Gaia* synthetic magnitudes to compute solar colours from a number of high fidelity flux calibrated spectra. From the CALSPEC library we use

a Kurucz model (sun\_mod\_001.fits) and a solar reference spectrum (sun\_reference\_stis\_002.fits) which combines absolute flux measurements from space and from the ground with a model spectrum longward of 9600 Å (Colina, Bohlin & Castelli 1996). We also use the Thuillier et al. (2004) spectra for two solar active levels (about half of a solar cycle), where in fact the difference between them is well below 1 mmag across the *Gaia* filters (hence we report only one set). Similarly, we can also use two spectra of Vega available on



**Table 2.** Extinction coefficients for *Gaia* filters. We report mean extinction coefficients  $\langle R_\zeta \rangle$  and a linear fit valid for  $5250 \text{ K} \leq T_{\text{eff}} \leq 7000 \text{ K}$ .

Filter	$\langle R_\zeta \rangle$	$R_\zeta = a_0 + T_4 (a_1 + a_2 T_4) + a_3 [\text{Fe}/\text{H}]$			
		$a_0$	$a_1$	$a_2$	$a_3$
<i>G</i>	2.740	1.4013	3.1406	-1.5626	-0.0101
$G_{\text{BP}}$	3.374	1.7895	4.2355	-2.7071	-0.0253
$G_{\text{RP}}$	2.035	1.8593	0.3985	-0.1771	0.0026

Based on the differences in the bolometric corrections for  $E(B - V) = 0.0$  and  $0.10$ , assuming  $\log g = 4.1$ ,  $-2.0 \leq [\text{Fe}/\text{H}] \leq +0.25$ , with  $[\alpha/\text{Fe}] = -0.4, 0.0$ , and  $0.4$  at each  $[\text{Fe}/\text{H}]$ . Note that  $T_4 = 10^{-4} T_{\text{eff}}$ . For a given nominal  $E(B - V)$ , the excess in any given  $\zeta - \eta$  colour is  $E(\zeta - \eta) = (R_\zeta - R_\eta)E(B - V)$ , and the attenuation for a magnitude  $m_\zeta$  is  $R_\zeta E(B - V)$ .

the CALSPEC library to estimate its magnitudes and colours (the Kurucz model `alpha_lyr_mod_002.fits`, and `alpha_lyr_stis_008.fits` which intermingles a Kurucz model with *HST*-STIS measurement across part of the *G* and  $G_{\text{BP}}$  bands). We remark that the *Gaia* system is tied to Vega (assigned to have 0 magnitudes in all bands) using a slightly different Kurucz model, and absolute flux calibration than CALSPEC. Hence, if we generate magnitudes following the *Gaia* formalism, and believe CALSPEC to better match the actual flux of Vega, it is not surprising that its magnitudes will be slightly different from 0. As it can be seen from Table 1 there is excellent agreement in the magnitudes and colours obtained from different spectral templates, with differences of only a few mmag, comparable to the precision reached by *Gaia*. At the level of 0.01 mag, it is thus possible to quote robust numbers for the Sun and Vega's magnitudes, independently of the adopted spectral template, and flavour of zero-points and transmission curves. In the Vega system we have  $G_\odot = -26.90$ , corresponding to an absolute magnitude of  $M_{G, \odot} = 4.67$ ,  $(G_{\text{BP}} - G)_\odot = 0.33$ ,  $(G - G_{\text{RP}})_\odot = 0.49$ , and  $(G_{\text{BP}} - G_{\text{RP}})_\odot = 0.82$  for the Sun, and  $G = 0.03$ ,  $(G_{\text{BP}} - G) = 0.005$ ,  $(G - G_{\text{RP}}) = 0.01$ , and  $(G_{\text{BP}} - G_{\text{RP}}) = 0.015$  for Vega.

Finally, in Table 2 we report extinction coefficients for the *Gaia* filters, both average and  $T_{\text{eff}}$ -dependent ones. Users interested in extinction coefficients at different values of temperature and/or metallicities can easily derive them from our routines.

## 5 CONCLUSIONS

*Gaia*, not least its photometry, will induce a paradigm shift in many areas of astronomy. However, to make full use of these data, colour predictions from stellar fluxes are mandatory, as well as control of systematics. We have expanded our previous investigations using MARCS stellar fluxes to include *Gaia*  $G_{\text{BP}}$ , *G*, and  $G_{\text{RP}}$  magnitudes. In doing so, we have explored the effects of implementing the two different sets of bandpasses and zero-points that have been released with *Gaia* DR2. Differences are typically of few mmag only. Further, we have generated a third set, which takes into account the *Gaia* Collaboration et al. (2018a) recommendations to provide the best match to observations. All of these sets are available as part of our interpolation package for users to explore. In examining the adopted zero-points, we uncovered a magnitude-dependent offset in *Gaia* *G* magnitudes. Albeit small, this trend amounts to 30 mmag over 10 magnitudes in the *G* band, which is larger than systematic effects at the 10 mmag level quoted by Evans et al. (2018). This offset is relatively small, but it potentially has a number of implications should *G* magnitudes be used, e.g. to calibrate distance indicators. Despite this offset, we regard *Gaia* magnitudes as an incredible success, delivering magnitudes for a billion sources with an accuracy within a few per cent of CALSPEC.

We also carried out an evaluation of the quality of our BCs and their impact on the luminosity error budget. *G* and  $G_{\text{RP}}$  magnitudes are typically better than  $G_{\text{BP}}$  in recovering bolometric fluxes, although averaging different bands is probably advisable whenever possible. Also, the systematic trend uncovered in *G* magnitudes does not impact bolometric fluxes too seriously, since uncertainties in adopted stellar parameters and the performance of the synthetic MARCS fluxes enter the error budget with a similar degree of uncertainty. All our previous interpolation routines and scripts have now been updated to include the *Gaia* system, and are available on GitHub ([github.com/casaluca/bolometric-corrections](https://github.com/casaluca/bolometric-corrections)). A description of the files and examples of their use can be found in appendix A of Paper II.

## ACKNOWLEDGEMENTS

We thank F. De Angeli and P. Montegriffo for useful correspondence, and the referee G. Busso for the same kindness. LC is the recipient of the ARC Future Fellowship FT160100402. Parts of this research were conducted by the ARC Centre of Excellence ASTRO 3D, through project number CE170100013. This work has made use of data from the European Space Agency (ESA) mission *Gaia* (<https://www.cosmos.esa.int/gaia>), processed by the *Gaia* Data Processing and Analysis Consortium (DPAC, <https://www.cosmos.esa.int/web/gaia/dpac/consortium>). Funding for the DPAC has been provided by national institutions, in particular the institutions participating in the *Gaia* Multilateral Agreement.

We thank Carme Jordi for pointing out that a trend in *Gaia* *G* magnitudes is also commented in Arenou et al. (arXiv:1804.09375) and Weiler et al. (arXiv:1805.08082)

## REFERENCES

- Altavilla G. et al., 2015, *Astrono. Nachr.*, 336, 515  
 Andrae R. et al., 2018, preprint (arXiv:1804.09374)  
 Bohlin R. C., 2014, *AJ*, 147, 127  
 Cardelli J. A., Clayton G. C., Mathis J. S., 1989, *ApJ*, 345, 245  
 Carrasco J. M. et al., 2016, *A&A*, 595, A7  
 Casagrande L., Vandenberg D. A., 2014, *MNRAS*, 444, 392  
 Casagrande L., Vandenberg D. A., 2018, *MNRAS*, 475, 5023  
 Casagrande L., Ramírez I., Meléndez J., Asplund M., 2012, *ApJ*, 761, 16  
 Colina L., Bohlin R. C., Castelli F., 1996, *AJ*, 112, 307  
 Evans D. W. et al., 2018, preprint (arXiv:1804.09368)  
 , *Gaia* Collaboration Brown A. G. A., Vallenari A., Prusti T., de Bruijne J. H. J., Babusiaux C., Bailer-Jones C. A. L., 2018a, preprint (arXiv:1804.09365)  
*Gaia* Collaboration et al., 2018b, preprint (arXiv:1804.09378)  
 Gustafsson B., Edvardsson B., Eriksson K., Jørgensen U. G., Nordlund Å., Plez B., 2008, *A&A*, 486, 951  
 Jordi C. et al., 2010, *A&A*, 523, A48

Meléndez J., Schuster W. J., Silva J. S., Ramírez I., Casagrande L.,  
Coelho P., 2010, *A&A*, 522, A98  
Pancino E. et al., 2012, *MNRAS*, 426, 1767  
Ramírez I. et al., 2012, *ApJ*, 752, 5  
Riello M. et al., 2018, preprint ([arXiv:1804.09367](https://arxiv.org/abs/1804.09367))

Thuillier G., Floyd L., Woods T. N., Cebula R., Hilsenrath M., Hersé M.,  
Labs D., 2004, *Adv. Space Res.*, 34, 256

This paper has been typeset from a  $\text{\TeX}/\text{\LaTeX}$  file prepared by the author.